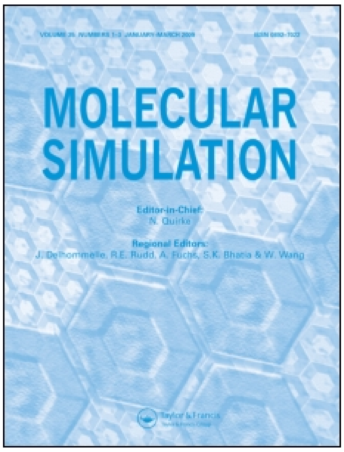

Molecular Simulation
Publication details, including instructions for authors and subscription information:
http://www.informaworld.com/smpp/title~content=t713644482

Biomimetic trinuclear copper mixed-valence systems: electronic and magnetic parameters from *ab initio* calculations

Carmen J. Calzado[a]
[a] Departamento de Química Física, Universidad de Sevilla, Sevilla, Spain

To cite this Article Calzado, Carmen J.(2009) 'Biomimetic trinuclear copper mixed-valence systems: electronic and magnetic parameters from *ab initio* calculations', Molecular Simulation, 35: 12, 1057 — 1066

To link to this Article: DOI: 10.1080/08927020902859074

URL: http://dx.doi.org/10.1080/08927020902859074

Molecular Simulation
Vol. 35, Nos. 12–13, October–November 2009, 1057–1066

Biomimetic trinuclear copper mixed-valence systems: electronic and magnetic parameters from *ab initio* calculations[†]

Carmen J. Calzado*

Departamento de Química Física, Universidad de Sevilla, c/Profesor García González, s/n., E-41012 Sevilla, Spain

(*Received 30 December 2008; final version received 23 February 2009*)

A series of *ab initio* quantum chemistry calculations on a trinuclear mixed-valence system $[(NH_3)_6Cu_3O_2]^{+3}$ has been performed in order to simultaneously evaluate its magnetic and electronic parameters, namely the magnetic coupling constants J_1 and J_2, the electron-transfer integrals t_1 and t_2, and the exchange-transfer terms h_1 and h_2. The procedure is based on the use of the effective Hamiltonian theory. The results evidence the presence of two ferromagnetic interactions in this compound, in good agreement with the behaviour found in the real system $[L_3Cu_3O_2]^{+3}$, where L = *N*-permethyl-(1*R*,2*R*)-cyclohexenediamine. Regarding electron-transfer terms, their values are about one order larger than the corresponding magnetic coupling constants, and essentially controlled by the direct interactions through the Cu d orbitals. The exchange-transfer terms are non-negligible, their amplitudes being similar to the J_1 constant.

Keywords: electron transfer; magnetic coupling; mixed-valence systems; biomimetic compounds

1. Introduction

The reduction of O_2 to give H_2O is one of the most relevant reactions in nature. In biological systems, this process is catalysed by the metalloenzymes, in particular by those containing active Cu sites [1–3]. In these enzymes, Cu exists in mononuclear and polynuclear configurations, although the nuclearity of the active site does not correlate directly with the type of reactivity (they can function as dioxygenases, monooxygenases and oxidases). Multicopper oxidase enzymes such as laccase, ascorbate oxidase or ceruloplasmin couple the four-electron reduction of O_2 to water with the one-electron oxidation of electron-rich substrates. The active site is a trinuclear Cu cluster, coupled to a Cu site (blue Cu site) 13 Å distant from the Cu_3 cluster, which provides the fourth electron [1–3].

Many efforts have been driven to understand the mechanism of this reaction. In particular, biochemical synthesis research has focus on the synthesis of biomimetic models that reproduce the topology and reactivity of the natural ones. Among them, Cole et al. [4] have reported the self-assembly synthesis of a trinuclear Cu/O_2 cluster, with a $Cu_3(\mu\text{-}O)_2$ core, of formula $[L_3Cu_3O_2]^{3+}$, L = *N*-permethyl-(1*R*,2*R*)-cyclohexenediamine (Figure 1). This compound represents the first example of 3:1 metal:O_2 stoichiometry in reactions between metal complexes and O_2. Generally, each of the Cu centres supplies only one electron. Therefore, one-, two- or four-electron reductions of O_2 has a 1:1, 2:1 or 4:1 metal:O_2 stoichiometry, respectively. In the case of the complex isolated by Cole et al., the four electrons are provided by three copper ions, which leads to a mixed-valence $[Cu_2(II)Cu(III)]$ system. X-ray structure analysis, UV–Vis spectra, NMR susceptibility, SQUID and MCD data [4,5] are all consistent with a description of a localised mixed-valence system (type II in Robin and Day classification), with two Cu(II) ions ferromagnetically coupled (an $S = 1$ electronic ground state), and one diamagnetic Cu(III) centre. The singlet–triplet splitting is only of $+14\,\mathrm{cm}^{-1}$. All three Cu centres have square-planar coordination environments, with shorter Cu—O bonds in the case of Cu(III) centre. The distortion does not arise from crystal packing effects since it is also present in solution [1], but it is related to a first-order Jahn–Teller effect. Root et al. [5] stated that this effect together with a weak electronic coupling can explain the localised nature of the mixed-valence system.

From a theoretical point of view, this system is a simplified model of polynuclear mixed-valence systems. Modelling the properties of them remains one of the open challenges in molecular magnetism, in particular, to elucidate the interplay between electronic delocalisation and magnetic interactions in these compounds [6]. Three types of interactions can be distinguished in the $[Cu_3O_2]^{+3}$ core, as shown in Figure 2, namely magnetic exchange coupling *J*, electron transfer, *t*, and the exchange-transfer term [7], *h*, also called singlet-displacement operator [8]. The magnetic exchange reverses the spin on two neighbour

---

[†] Dedicated to the memory of José Antonio Mejías, a talented scientist, an enthusiastic researcher and an honest person

*Email: calzado@us.es

ISSN 0892-7022 print/ISSN 1029-0435 online

DOI: 10.1080/08927020902859074
http://www.informaworld.com

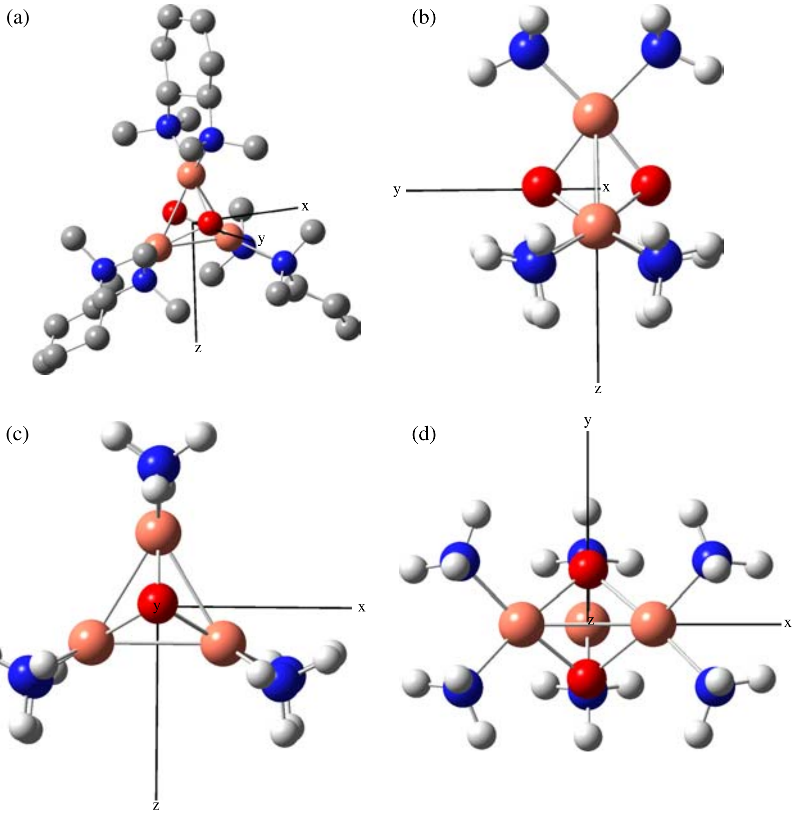

Figure 1. Crystal structure of $[L_3Cu_3O_2]^{+3}$ system. (a) Structure of unit A from Cambridge Structural Database. Hydrogen atoms are not shown. (b, c, d) Three views (along *x*-, *y*- and *z*-axes, respectively) of the corresponding model structure employed on the calculations, where L ligands are replaced by NH_3 groups.

sites, the electron-transfer constant moves the electron to a neighbour hole and the exchange-transfer term moves the pair of electrons, coupled in a singlet, towards a hole placed in a neighbour position. Thus, a singlet on sites *a* and *c*, the site *b* containing a hole, is displaced to the positions *a* and *b*, the hole being in *c*.

Different theoretical works have tried to elucidate the origin of the ferromagnetic coupling [5,9–11] and quantify the stabilisation produced by the Jahn–Teller distortion [5,12]. Density functional theory (DFT)-based calculations on a model system where L ligands are replaced by NH_3 groups correctly reproduce the triplet ground state, but largely overestimate the triplet–singlet separation ($J = 878\ \mathrm{cm}^{-1}$[5], $J = 72–550\ \mathrm{cm}^{-1}$ [9]; $J = 231\ \mathrm{cm}^{-1}$[10]; $J = 806–2934\ \mathrm{cm}^{-1}$ [11]). Any evaluation of the electronic coupling has been reported, except a rude estimation from the energies of the magnetic orbitals [5], nor of the exchange-transfer term.

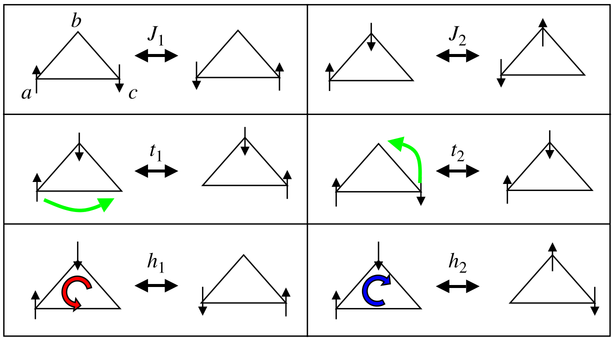

Figure 2. Magnetic coupling, electron-transfer and singlet-displacement terms in Cu_3O_2 core.

In this field, an alternative to DFT-based methods lies in the use of extended configuration interaction (CI) approaches, in particular difference-dedicated CI (DDCI) calculations [13]. The main advantage of this method is to take into account dynamical correlation effects at a reduced computational cost compared to a conventional CI calculation. In fact, the central idea is to obtain the energies and eigenvectors of the desired states from a truncated CI expansion, where all the double excitations from two inactive occupied orbitals towards two inactive virtual ones (the most numerous ones) are eliminated, since they contribute neither to the magnetic coupling constant nor to the electron-transfer integrals. The method provides estimates of the exchange coupling constants and hopping integrals in good agreement with the experimental values

Table 1. Geometrical parameters of the two non-equivalent clusters on the unit cell.

Cluster	bond lengths (Å)					bond angles (°)		dihedral angles (°)			
	Cu_a—Cu_b	Cu_a—Cu_c	Cu_a—O	Cu_b—O	O—O	Cu_aOCu_b	Cu_aOCu_c	NCu_aNO	NCu_bNO	Cu_aOOCu_b	Cu_aOOCu_c
A	2.652	2.719	1.966	1.839	2.260	88.3 89.2	88.3	177.5 −172.7	177.1 −179.6	121.1	−117.8
B	2.634	2.704	1.977	1.831	2.363	87.5 86.6	85.5	161.3 −176.3	164.1 −178.8	122.5	−114.9

both in molecular and periodic systems [14–24]. This approach has also been recently used to study a series of (μ_3-hydroxo)- and (μ_3-oxo)-bridged trinuclear Cu(II) models by Chalupsk et al. [25] and Le Guennic et al. [26].

The aim of the present work is to evaluate all the electronic and magnetic parameters governing the properties of this system from *ab initio* quantum chemistry calculations. DDCI method is employed to determine the energies and wavefunctions of the low-lying states of the system. Combined with the effective Hamiltonian theory, it is possible to simultaneously extract the electronic and magnetic coupling constants and the exchange-transfer terms. Also a direct estimate of the relative stability of the local forms is obtained as well as a measure of the on-site Coulomb energies ($U_a = U_c$, U_b).

The manuscript is organised as follows: the real system and the model employed in calculations are described in Section 2 and the method in Section 3. Results are reported in Section 4, and main conclusions are summarised in Section 5.

2. Description of the real and model systems

The real system contains two non-equivalent $[L_3Cu_3O_2]^{+3}$ clusters for each unit cell, both with C_2 symmetry. Table 1 collects the main geometrical parameters of both clusters (A and B), the main difference being the O—O distance (2.26 and 2.36 Å, respectively). We have employed the experimental geometries from X-ray diffraction data for this system, and both inequivalent structures have been analysed. Any symmetry constraint has been imposed, at difference with previous theoretical works. In order to reduce the computational cost, the external L ligands are replaced by NH_3 groups, maintaining the original position of N atoms, where the H atoms are placed in such a way the C_2 axis is preserved. This change could affect the amplitude of the interactions under consideration, but only a minor effect is expected, at least for *J*, as suggested in previous works, where the impact of external ligands on *J* has been considered [11,20]. Figure 1 represents the structure A of the real system and three views of the corresponding model.

In all the calculations, core electrons of Cu, O and N atoms were replaced with effective core potentials, where the (9s6p6d)/[3s3p4d] set was used for the valence electrons of Cu atoms, (5s6p1d)/[2s3p1d] set for O atoms and (5s5p1d)/[2s3p1d] set for N atoms [27]. A double-zeta basis set has been employed for H atoms. CI calculations are performed by means of CASDI code [28] on the basis of the ground triplet molecular orbitals.

3. How to obtain the amplitude of the coupling constants

3.1 Identification of the effective parameters

The mixed-valence $[Cu_3O_2]^{+3}$ core contains two Cu(II) atoms and a single Cu(III) one. As well known, a Cu(II) atom in a pseudo-square planar coordination places the unpaired electron on a molecular orbital, essentially Cu dx^2-y^2 but with tails on the four neighbour atoms. Let us call a, b and c these unpaired orbitals, a and c being related by a C_2 axis.

In order to extract the effective parameters, let us consider the neutral determinants with $S_z=0$ that can be built on the basis of the localised orbitals: $\{|a\bar{b}\rangle, |\bar{a}b\rangle, |b\bar{c}\rangle, |\bar{b}c\rangle, |a\bar{c}\rangle, |\bar{a}c\rangle\}$. They constitute the model space $\mathbb{S}$. The corresponding ionic determinants $\{|a\bar{a}\rangle, |b\bar{b}\rangle, |c\bar{c}\rangle\}$ are high in energy, due to the on-site Coulomb repulsion $U, U_m = E_{m\bar{m}} - E_{m\bar{n}}$ $\{m,n\}=\{a,b,c\}$. The Hamiltonian spanned by such a model space can be written as:

$$\begin{array}{cccccc}
|a\bar{b}\rangle & |\bar{a}b\rangle & |b\bar{c}\rangle & |\bar{b}c\rangle & |a\bar{c}\rangle & |\bar{a}c\rangle \\
\hline
J_2 & -J_2 & h_2 & -t_1-h_2 & -t_2-h_1 & h_1 \\
 & J_2 & -t_1-h_2 & h_2 & h_1 & -t_2-h_1 \\
 & & J_2 & -J_2 & t_2+h_1 & -h_1 \\
 & & & J_2 & -h_1 & t_2+h_1 \\
 & & & & J_1+\varepsilon & -J_1 \\
 & & & & & J_1+\varepsilon
\end{array} \qquad (1)$$

or on the basis of their six combinations:

$$\begin{array}{cccccc}
|S_{ab}\rangle & |S_{bc}\rangle & |S_{ac}\rangle & |T_{ab}\rangle & |T_{bc}\rangle & |T_{ac}\rangle \\
\hline
2J_2 & t_1+2h_2 & -t_2-2h_1 & 0 & 0 & 0 \\
 & 2J_2 & t_2+2h_1 & 0 & 0 & 0 \\
 & & 2J_1+\varepsilon & 0 & 0 & 0 \\
 & & & 0 & -t_1 & -t_2 \\
 & & & & 0 & t_2 \\
 & & & & & \varepsilon \\
\hline
\end{array} \qquad (2)$$

where $|S_{mn}\rangle = (|m\bar{n}\rangle - |\bar{m}n\rangle)/\sqrt{2}$ and $|T_{mn}\rangle = (|m\bar{n}\rangle + |\bar{m}n\rangle)/\sqrt{2}$ for $\{m,n\}=\{a,b,c\}$. The zero of energy is that of the triplet states $|T_{ab}\rangle$ or $|T_{bc}\rangle$. The term ε represents the stabilisation of the hole localised on site b with respect to those situations, where the hole is placed on site a or c; that is, it quantifies the extension of the Jahn–Teller distortion. Since the Cu atoms form an isosceles triangle, two different magnetic coupling constants can be distinguished, J_1 between sites a and c and J_2 between sites $a(c)$ and b (Figure 2). These constants are defined according to the Heisenberg Hamiltonian: $\hat{H}_{\text{Heis}} = -2J_{ij}(\hat{S}_i\hat{S}_j - 1/4)$, where the singlet–triplet separation is equal to $2J$, and then J is positive for a ferromagnetic system. Similarly, two different electron-transfer integrals can be identified, as shown in Figure 2. The term t_1 couples the electron delocalisation between sites a and c, and t_2 permits the *direct* transfer between sites a and b or b and c. Notice that the sign of the overlap of Cu$_a$ d and Cu$_b$ d orbitals ($\propto t_{ab}$) is opposite to that of Cu$_b$ and Cu$_c$ orbitals ($\propto t_{bc}$; see Scheme in Table 2). Then $t_2 = t_{ab} = -t_{bc}$. For the same reason, it is expected that t_1 and t_2 have opposite sign. Regarding the exchange-transfer term, the operator h_1 produces an anticlockwise singlet displacement [8], in such a way that, a singlet on sites a and b, with spins up and down, respectively, is displaced to sites c (up) and a (down). This movement can be conceived as a two-step pathway (Figure 3), where firstly the electron in site b is transferred to site a, followed by a second transfer towards c. This effect scales as $t_2t_1/(U_a+\varepsilon)$. The coupling of $|\bar{a}c\rangle$ with $|a\bar{b}\rangle$ is also equal to h_1, but in this case the displacement is clockwise. On the other hand, the operator h_2 controls the clockwise movement of the singlet: a singlet on sites a and b is displaced to sites b and c. As for h_1, this effect can be identified with a two-step pathway, involving the ionic $|b\bar{b}\rangle$ determinant, scaling as $(t_2)^2/U_b$. Moreover, the term h_1 contributes to the coupling between the $|a\bar{b}\rangle$ and $|a\bar{c}\rangle$ determinants, since it represents an indirect pathway for the electron transfer between sites b and c (Figure 4). The same holds for the h_2 term and the electron transfer between sites a and b [8].

Table 2. Magnetic exchange, electron-transfer and singlet-displacement terms (in cm^{-1}) for the two $[L_3Cu_3O_2]^{+3}$ clusters in the unit cell.

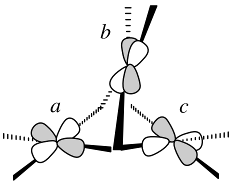

Cluster	J_1	J_2	t_1	t_2	h_1	h_2	ε	U_a	U_b
A	39.6	128.4	540.3	−1466.7	33.2	47.4	−3.617	6.58	5.62
B	46.3	122.7	378.8	−1198.7	5.7[a]	31.6	−3.933	–[a]	5.64

The stabilisation energy ε and on-site Coulomb energies, U_a and U_b, values are in eV.

[a] This value is on the limit of accuracy of the procedure, and it must be dealt with caution: consequently, the corresponding U_a value is not reported.

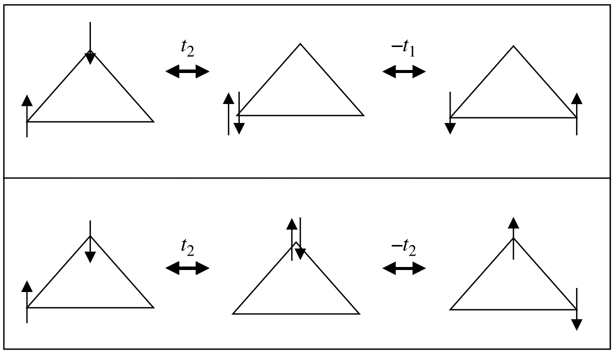

Figure 3. Pathways showing the singlet-displacement operators, h_1 (top) and h_2 (bottom).

In summary, the magnetic and electronic constants, *J*, *t* and *h*, correspond to coupling terms of a Hamiltonian built on the basis of the neutral determinants resulting from the distribution of two electrons on three active orbitals, *a*, *b* and *c*. The next question is how these matrix elements can be isolated from the energies and wavefunctions provided by a set of CI calculations.

3.2 The machinery

The diagonalisation of the Hamiltonian matrix on the basis of the neutral determinants (Equation (1) or their corresponding combinations in Equation (2)) gives six eigenstates: three singlet and three triplet states, where two singlet (triplet) states are of symmetry A (B) and one singlet (triplet) state of symmetry B (A). Their energies can be written from the basic parameters as:

$$\begin{aligned} E_{S_3} &= 2J_2 + t_1 + 2h_2 & E_{T_2} &= -t_1 \\ E_{S_1,S_2} &= \left((M+N) \mp \sqrt{(M-N)^2 + 8(t_2+2h_1)^2}\right)/2 & E_{T_1,T_3} &= \left((t_1+\varepsilon) \mp \sqrt{(t_1-\varepsilon)^2 + 8t_2^2}\right)/2 \end{aligned} \qquad (3)$$

where $M = 2J_2 - t_1 - 2h_2$ and $N = 2J_1 + \varepsilon$. Notice that the singlet-displacement terms appear only on the singlet eigenvalues, since they stabilise the singlet but not the triplet states. The resulting spectrum depends on the relative values of the seven parameters involved. (Here, in order to simplify the discussion of the results, the labels of these states correspond to the distribution obtained from our CI calculations. That is, it makes use of *a posteriori* information, once the wavefunctions have been analysed. Otherwise, there is no way to sort these states, prior to the determination of the effective parameters). Since there are only five energy differences, it is clear that these parameters cannot be univocally defined just from the spectrum. Also the information contained on the wavefunctions is necessary, and this is the goal of the effective Hamiltonian theory. This strategy has been previously used in the study of magnetic systems as well as the evaluation of electron-transfer constants in mixed-valence systems [14,21–24,29–34]. A detailed description of the method can be found in [8,22], only the most striking points are provided here.

Let us consider the model space $\mathbb{S} = \left\{|a\bar{b}\rangle, |\bar{a}b\rangle, |b\bar{c}\rangle, |\bar{b}c\rangle, |a\bar{c}\rangle, |\bar{a}c\rangle\right\}$ spanned by the six neutral determinants. Also it is possible to use their six combinations: $\{|S_{ab}\rangle, |S_{bc}\rangle, |S_{ac}\rangle, |T_{ab}\rangle, |T_{bc}\rangle, |T_{ac}\rangle\}$. Its projector is:

$$\hat{P}_S = \sum_{i \in S} |\phi_i\rangle\langle\phi_i| \qquad (4)$$

From DDCI calculations, we can obtain *six* approximated solutions $\{|\Phi_k\rangle, k = 1,6\}$ to the exact Hamiltonian, which hereafter will be considered as exact. These solutions have the largest components in the model space $\mathbb{S}$ with energies E_k. They constitute the target space $\mathbb{S}'$. Now we define an effective Hamiltonian in $\mathbb{S}$ such as its *six* eigenvalues are exact, then equal to E_k, and its eigenvectors are projections of the corresponding exact eigenvectors in the model space. This is the definition of Bloch effective Hamiltonian [35]:

$$\hat{H}_{\text{eff}}^{\text{Bloch}} \left|\hat{P}_S \Phi_k\right\rangle = E_k \left|\hat{P}_S \Phi_k\right\rangle. \qquad (5)$$

This basic equation leads to the spectral definition of the Bloch effective Hamiltonian [35]:

$$\hat{H}_{\text{eff}}^{\text{Bloch}} = \sum_{k=1,6} \left|\hat{P}_S \Phi_k\right\rangle E_k \left\langle \hat{P}_S \Phi_k^{\dagger}\right|, \qquad (6)$$

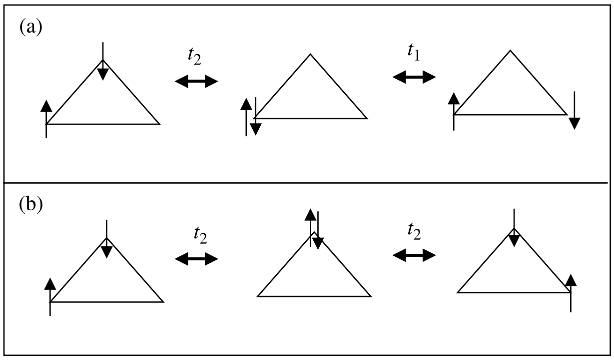

Figure 4. Pathways showing the singlet-displacement contributions to the transfer of an electron between two neighbour sites. (a) Coupling between the $|a\bar{b}\rangle$ and $|a\bar{c}\rangle$ determinants mediated by the h_1 term, and (b) coupling between the $|a\bar{b}\rangle$ and $|\bar{b}c\rangle$ determinants by the h_2 term.

where $\left|\hat{P}_S\Phi_k^\dagger\right\rangle$ represents the biorthogonal vector associated to $\left|\hat{P}_S\Phi_k\right\rangle$, defined by:

$$\left|\hat{P}_S\Phi_k^\dagger\right\rangle = S^{-1}\left|\hat{P}_S\Phi_k\right\rangle, \tag{7}$$

where S is the overlap matrix of the projections of the solutions of the exact Hamiltonian onto the model space:

$$S_{ij} = \left\langle\hat{P}_S\Phi_i\middle|\hat{P}_S\Phi_j\right\rangle. \tag{8}$$

In our case, all the calculations have been carried out in the C_2 symmetry group. The active orbitals are the symmetry-adapted combinations of the localised a, b and c orbitals:

$$\begin{aligned} g &= \frac{a+c}{\sqrt{2}} \\ &\left.\begin{aligned} u &= \alpha\big((a-c)/\sqrt{2}\big) + \beta b \\ u' &= \beta\big((a-c)/\sqrt{2}\big) - \alpha b \end{aligned}\right\}\alpha > \beta > 0, \end{aligned} \tag{9}$$

where g belongs to the A irreducible representation and u and u' to the B one. Then prior to perform the projections of the CI wavefunctions on the model space, we need to determine the α/β ratio by a localising unitary transformation. Next, the normalised projections on the model space can be written as:

$$\begin{aligned} \left|\hat{P}_S{}^1\Phi_1\right\rangle &= -\delta\big(|S_{ab}\rangle - |S_{bc}\rangle\big) + \gamma|S_{ac}\rangle \quad \gamma > \delta > 0 \\ \left|\hat{P}_S{}^1\Phi_2\right\rangle &= \gamma'\big(|S_{ab}\rangle - |S_{bc}\rangle\big) + \delta'|S_{ac}\rangle \quad \gamma' > \delta' > 0 \\ \left|\hat{P}_S{}^1\Phi_3\right\rangle &= \frac{1}{\sqrt{2}}\big(|S_{ab}\rangle + |S_{bc}\rangle\big) \\ \left|\hat{P}_S{}^3\Phi_1\right\rangle &= -\delta''\big(|T_{ab}\rangle - |T_{bc}\rangle\big) + \gamma''|T_{ac}\rangle \quad \gamma'' > \delta'' > 0 \\ \left|\hat{P}_S{}^3\Phi_2\right\rangle &= \frac{1}{\sqrt{2}}\big(|T_{ab}\rangle + |T_{bc}\rangle\big) \\ \left|\hat{P}_S{}^3\Phi_3\right\rangle &= \gamma'''\big(|T_{ab}\rangle - |T_{bc}\rangle\big) + \delta'''|T_{ac}\rangle \quad \gamma''' > \delta''' > 0, \end{aligned} \tag{10}$$

where the equivalences between the $|S_{ab}\rangle$ $\big(|T_{ab}\rangle\big)$ and $|S_{bc}\rangle$ $\big(|T_{bc}\rangle\big)$ combinations are due to symmetric reasons, imposed by the structure of the cluster. The non-null elements of the overlap matrix are:

$$\begin{aligned} \left\langle\hat{P}_S{}^1\Phi_2\middle|\hat{P}_S{}^1\Phi_1\right\rangle &= -\delta\gamma' + \gamma\delta' = p \\ \left\langle\hat{P}_S{}^3\Phi_3\middle|\hat{P}_S{}^3\Phi_1\right\rangle &= -\delta''\gamma''' + \gamma''\delta''' = q. \end{aligned} \tag{11}$$

The biorthogonal vectors are then defined by:

$$\begin{aligned} \left|\hat{P}_S{}^1\Phi_1^\dagger\right\rangle &= \frac{1}{1-p^2}\left(\left|\hat{P}_S{}^1\Phi_1\right\rangle - p\left|\hat{P}_S{}^1\Phi_2\right\rangle\right) \\ \left|\hat{P}_S{}^1\Phi_2^\dagger\right\rangle &= \frac{1}{1-p^2}\left(-p\left|\hat{P}_S{}^1\Phi_1\right\rangle + \left|\hat{P}_S{}^1\Phi_2\right\rangle\right) \\ \left|\hat{P}_S{}^3\Phi_1^\dagger\right\rangle &= \frac{1}{1-q^2}\left(\left|\hat{P}_S{}^3\Phi_1\right\rangle - q\left|\hat{P}_S{}^3\Phi_3\right\rangle\right) \\ \left|\hat{P}_S{}^3\Phi_3^\dagger\right\rangle &= \frac{1}{1-q^2}\left(-q\left|\hat{P}_S{}^3\Phi_1\right\rangle + \left|\hat{P}_S{}^3\Phi_3\right\rangle\right) \\ \left|\hat{P}_S{}^1\Phi_3^\dagger\right\rangle &= \left|\hat{P}_S{}^1\Phi_3\right\rangle; \left|\hat{P}_S{}^3\Phi_2^\dagger\right\rangle = \left|\hat{P}_S{}^3\Phi_2\right\rangle \end{aligned} \tag{12}$$

and now, the effective elements can be evaluated from the spectral definition of the Bloch Hamiltonian. For instance, the hopping integral t_2 can be obtained from:

$$\begin{aligned} t_2 = \left\langle T_{bc}\middle|\hat{H}_{\text{eff}}\middle|T_{ac}\right\rangle &= \left\langle T_{bc}\middle|\hat{P}_S{}^3\Phi_1\right\rangle E_{T_1}\left\langle\hat{P}_S{}^3\Phi_1^\dagger\middle|T_{ac}\right\rangle \\ &+ \left\langle T_{bc}\middle|\hat{P}_S{}^3\Phi_2\right\rangle E_{T_2}\left\langle\hat{P}_S{}^3\Phi_2^\dagger\middle|T_{ac}\right\rangle \\ &+ \left\langle T_{bc}\middle|\hat{P}_S{}^3\Phi_3\right\rangle E_{T_3}\left\langle\hat{P}_S{}^3\Phi_3^\dagger\middle|T_{ac}\right\rangle \end{aligned} \tag{13}$$

and in a similar way for the rest of parameters. Notice that due to the non-orthogonality of the projections $\left|\hat{P}_S\Phi_k\right\rangle$, the Bloch Hamiltonian is non-Hermitian. Consequently, the matrix element H_{ij} may be different from H_{ji} and in that case the mean value is reported.

4. Results

All the calculations have been performed at DDCI level on the basis of the molecular orbitals of the lowest triplet state. Figure 5 shows two views of the active u and u' orbitals for cluster A, which present a pronounced degree of localisation ($\alpha = 0.99731$ in Equation (9)). A very similar description is obtained for cluster B, where $\alpha = 0.99838$.

Figure 6 reports the spectrum of the six low-lying states of cluster A, as well as their normalised projections on the model space. The six states are distributed in two sets, separated by a gap of around 29,000 cm^{-1}, which is approximately the amplitude of ε, i.e. the relative stabilisation of the hole localised on site b with respect to those situations, where the hole is placed on site a or c.

The analysis of the DDCI wavefunctions of both clusters shows that the ground state corresponds to a triplet state, largely dominated by the $|T_{ac}\rangle$ component (99% of the projected wavefunction is represented by this contribution). The two active electrons are localised on the two symmetry-equivalent Cu atoms, Cu_a and Cu_c. This description is in agreement with the localised

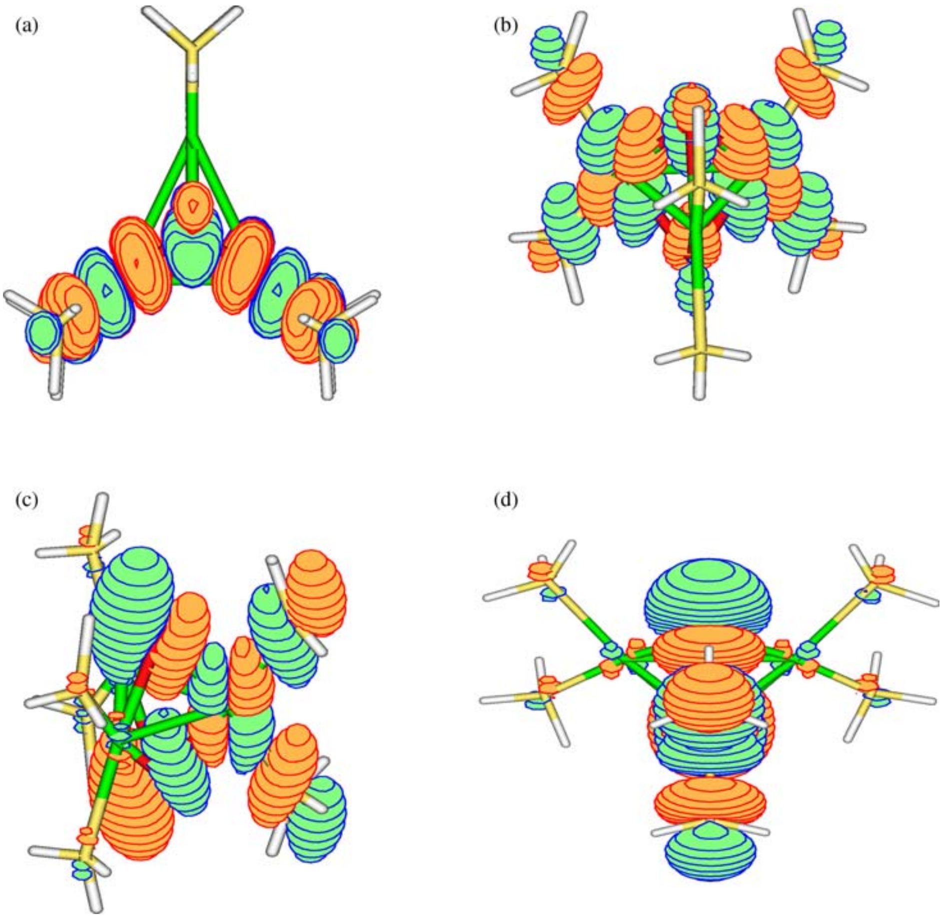

Figure 5. Active orbitals u and u' for cluster A. (a, b) Views of active u orbital along y- and z-axes, respectively. (c, d) Views of active u' orbital along x- and z-axes, respectively.

mixed-valence nature of this system, supported by all the available experimental data. The lowest excited state is the corresponding singlet state, essentially represented by the $|S_{ac}\rangle$ component (Figure 6). That is, the two lowest states of the trinuclear system are practically equivalent to those resulting from a binuclear complex, with two electrons distributed on two sites. In this particular case, it could be pertinent to evaluate the magnetic coupling constant between sites a and c, J_1, directly from the energy difference between these two states. The resulting values are $J_1 = 43.7\,\mathrm{cm}^{-1}$ for cluster A, and $J_1 = 46.3\,\mathrm{cm}^{-1}$ for cluster B. These amplitudes are overestimated with respect to the experimental value (experimental singlet–triplet separation of $+14\,\mathrm{cm}^{-1}$), but they are in really better agreement that any of the previous evaluations based on DFT calculations [5,9,10,11]. Moreover, it is worth to notice that several works have recently shown that DDCI approach slightly overestimates the ferromagnetic coupling constants [24,32,36], and that spin-orbit effects are not taken into

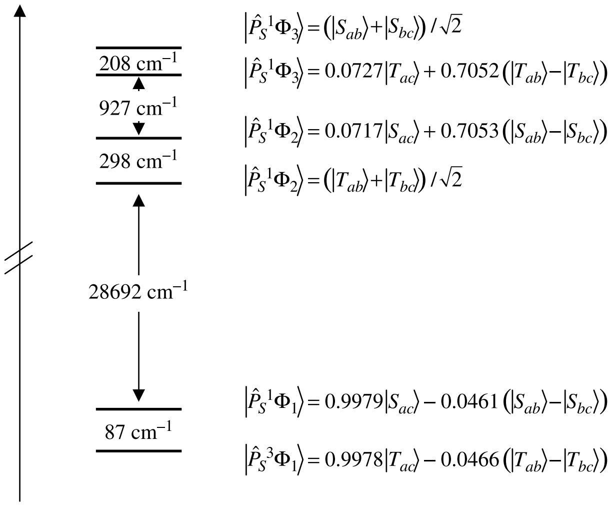

Figure 6. Spectrum of the $[L_3Cu_3O_2]^{+3}$ system (cluster A), representing the six low-lying states and their normalised projections on the model space.

account in our calculations, which can also affect the singlet–triplet separation.

The four remaining states correspond to the symmetric and antisymmetric combinations of the $|S_{ab}\rangle$ $\left(|T_{ab}\rangle\right)$ and $|S_{bc}\rangle$ $\left(|T_{bc}\rangle\right)$ components. So, the rest of parameters cannot be evaluated directly from energy differences, and can only be determined with the help of effective Hamiltonians. It is important to mention that the use of effective Hamiltonian theory is a general procedure, which can be employed independently of the degree of localisation of the low-lying states, while the evaluation of the magnetic coupling constant from the energy difference is possible only due to the fact that both the lowest singlet and ground triplet states present quite large weight on a unique component ($|S_{ac}\rangle$ and $|T_{ac}\rangle$ components, respectively). The so-obtained values of the effective parameters J, t and h for clusters A and B are reported in Table 2. Also shown are the stabilisation energy ε, and the on-site Coulomb repulsion terms, U_a and U_b. As expected, the effective parameters for both clusters are quite similar in values and trends, and the J_1 values are in good agreement with those extracted from the energy differences. The energies of the lowest singlet and triplet states on the basis of the effective parameters are shown in Equation (3) as E_{S1} and E_{T1}. Both of them depend not only on J_1 but also on the rest of parameters. The fact that the singlet–triplet energy difference matches the $2J_1$ value is due to a compensation of the other parameters, and a verification of the localised nature of the two lowest states.

The ferromagnetic nature of the magnetic coupling constants is in agreement with the Goodenough and Kanamori rules [37] and magnetostructural relationships reported by Ruiz et al. [38] for binuclear oxo-bridged Cu(II) complexes. They predict ferromagnetic coupling for those systems with Cu—O—Cu bridges close to 90°. However, in this system, the main structural parameter governing the amplitude and sign of the different parameters is not the Cu—O—Cu bond angle, but the dihedral Cu—O—O—Cu angle and the Cu—Cu distance. The small dihedral Cu—O—O—Cu angles produce an inefficient overlap of the oxygen bridging atoms with the Cu 3d orbitals. O 2p orbitals are practically orthogonal to the plane containing Cu$_a$ and Cu$_c$ atoms (Figure 5(c) and (d)). This particular structure has an important impact on the nature and amplitude of the interactions.

Regarding the magnetic coupling, two contributions with opposite signs can be distinguished: $J = J_{\mathrm{F}} + J_{\mathrm{AF}} = 2K - 4t^2/U$, where the former term corresponds to the direct exchange that produces a ferromagnetic contribution, the latter term takes into account the coupling through the bridging ligands. The geometry of the system imposes a reduced contribution of the oxygen atoms on the coupling, the main mechanism being the direct interaction between the Cu atoms, instead of the superexchange through the bridging atoms. Then, the smaller the Cu—Cu distance, the larger the direct exchange is, and consequently, the ferromagnetic contribution governs the interaction. This explains why J_2 is larger than J_1 for each cluster.

Also the electron-transfer integrals follow this trend. The amplitude of the electronic coupling constants are essentially controlled by the Cu—Cu distance, that is, by the through-space component of the electronic coupling, while the through-bond one plays a minor role. Consequently, t_2 is larger than t_1, since the Cu$_a$—Cu$_\mathrm{b}$ distance is smaller than the Cu$_a$—Cu$_c$ one. Moreover, the signs are different, due to the d–d overlap, which is positive for d orbitals in sites a and b, but negative for those in sites a and c, as shown in the inset in Table 2. Also notice that $t_2 = t_{ab} = -t_{bc}$ for the same reason. As mentioned above, the reported t_2 in Table 2 is the mean value of the effective matrix elements $\langle T_{bc}|\hat{H}_{\mathrm{eff}}|T_{ac}\rangle$ and $\langle T_{ac}|\hat{H}_{\mathrm{eff}}|T_{bc}\rangle$, which can be different due to the non-hermiticity of the Bloch Hamiltonian. For cluster A, $\langle T_{bc}|\hat{H}_{\mathrm{eff}}|T_{ac}\rangle = 1394\,\mathrm{cm}^{-1}$, while $\langle T_{ac}|\hat{H}_{\mathrm{eff}}|T_{bc}\rangle = 1539\,\mathrm{cm}^{-1}$, which represents only a deviation of 5% with respect to the mean value $t_2 = 1467\,\mathrm{cm}^{-1}$. A slightly larger deviation (12%) is found for cluster B, where $\langle T_{bc}|\hat{H}_{\mathrm{eff}}|T_{ac}\rangle = 1340\,\mathrm{cm}^{-1}$ and $\langle T_{ac}|\hat{H}_{\mathrm{eff}}|T_{bc}\rangle = 1057\,\mathrm{cm}^{-1}$.

Since the two lowest states are strongly localised on the $|T_{ac}\rangle$ and $|S_{ac}\rangle$ components, it is possible to obtain an estimate of the direct exchange between sites a and c, K_{ac}, from the composition of the lowest singlet wavefunction, the singlet–triplet energy difference and the electron-transfer integral $t_{ac} = t_1$ (see a detailed description of the procedure in Ref. [22]). The so-obtained $2K_{ac}$ value is $106.5\,\mathrm{cm}^{-1}$ for cluster A and $101.2\,\mathrm{cm}^{-1}$ for cluster B. Then, the antiferromagnetic contribution is only 27.3 and $8.6\,\mathrm{cm}^{-1}$, respectively, the global constant being governed by the direct interaction between sites a and c.

On the other hand, the singlet-displacement terms are non-negligible, being of the same order than the J_1 magnetic coupling constants as suggested by Blondin and Girerd [7]. Since $h_1 = t_2 t_1/(U_a + \varepsilon)$ and $h_2 = t_2^2/U_b$, it is possible to evaluate the on-site Coulomb repulsion terms from the singlet-displacement and hopping integral amplitudes, the so-obtained value being around 6 eV, with only small differences between sites $a(c)$ and b. For cluster B, the reported value for h_1 must be dealt with caution since it is on the limit of accuracy of the procedure. Consequently, the corresponding U_a value is not reported.

Comparing the parameters for clusters A and B, the main differences come from the hopping integrals and the stabilisation energy ε. Even when the geometrical parameters for A and B are quite close, the Jahn–Teller distortion seems to be more efficient from an energetic point of view for cluster B than for A, with a differential stabilisation of 0.3 eV. This suggests that the degree of localisation on cluster B is larger than that in cluster A, which is in line with smaller electronic coupling constants (hopping integrals) for B than A.

5. Conclusions

The magnetic and electronic local parameters acting on a mixed-valence [Cu_2(II)Cu(III)] compound are evaluated by means of extended CI calculations and the use of the effective Hamiltonian theory. The results confirm the ferromagnetic nature of the system, and provide estimates of the electron-transfer terms and the singlet-displacement operators. Also the extension of the Jahn–Teller distortion is quantified. The strategy is completely general, and can be employed independently of the degree of localisation of the system. Since all the information is mapped on a model Hamiltonian, it is possible to check the presence of additional interactions (with non-null elements on the Hamiltonian matrix), avoiding any possible bias due to the choice of a too limited set of effective parameters. Works are in progress in order to elucidate the impact of the nature of the bridging ligand on the magnetic properties of this complex.

Acknowledgements

I would like to deeply acknowledge Dr Juan Antonio Anta and Dr Sofía Calero for taking the initiative to edit this special issue in honour of Dr José Antonio Mejías, as well as for their invitation to participate in it. I am very grateful to E. Iglesias also for his careful reading of this manuscript as a way to pay homage to his friend José Antonio.

References

[1] L.M. Mirica, X. Ottenwaelder, and T.D.P. Stack, *Structure and spectroscopy of copper-dioxygen complexes*, Chem. Rev. 104 (2004), pp. 1013–1045.

[2] E.I. Solomon, U.M. Sundaram, and T.E. Machonkin, *Multicopper oxidases and oxygenases*, Chem. Rev. 96 (1996), pp. 2563–2606.

[3] E.I. Solomon, A.J. Augustine, and J. Yoon, *O_2 reduction to H_2O by the multicopper oxidases*, Dalton Trans. 30 (2008), pp. 3921–3932.

[4] A.P. Cole, D.E. Root, P. Mukherjee, E.I. Solomon, and T.D.P. Stack, *A trinuclear intermediate in the copper-mediated reduction of O_2: four electrons from three coppers*, Science 273 (1996), pp. 1848–1850.

[5] D.E. Root, M.J. Henson, T. Machonkin, P. Mukherjee, T.D.P. Stack, and E.I. Solomon, *Electronic and geometric structure of a trinuclear mixed-valence copper(II,II,III) cluster*, J. Am. Chem. Soc. 120 (1998), pp. 4982–4990.

[6] J.S. Miller and M. Drillon (eds.), *Magnetism: Molecules to Materials II. Nanosized Magnetic Materials*, Weinheim, Wiley-VCH, 2002.

[7] G. Blondin and J.J. Girerd, *Interplay of electron exchange and electron transfer in metal polynuclear complexes in proteins or chemical models*, Chem. Rev. 90 (1990), pp. 1359–1376.

[8] C.J. Calzado and J.P. Malrieu, *Proposal of an extended t–J Hamiltonian for high-Tc cuprates from* ab initio *calculations on embedded clusters*, Phys. Rev. B 63 (2001), 214520.

[9] I. Ciofini and C.A. Daul, *DFT calculations of molecular magnetic properties of coordination compounds*, Coord. Chem. Rev. 238–239 (2003), pp. 187–209.

[10] E.C. Brown, J.T. York, W.E. Antholine, E. Ruiz, S. Alvarez, and W.B. Tolmana, *$[Cu_3(\mu\text{-}S)_2]^{3+}$ clusters supported by N-donor ligands: progress towards a synthetic model of the catalytic site of nitrous oxide reductase*, J. Am. Chem. Soc. 127 (2005), pp. 13752–13753.

[11] C. Daul, S. Fernandez-Ceballos, I. Ciofini, C. Rauzy, and C.-W. Schläpfer, *A novel density functional study of the ground state properties of a localized trinuclear copper(II,II,III) mixed-valence system*, Chem. Eur. J. 8 (2002), pp. 4392–4401.

[12] A. Berces, *The self-assembly of inorganic mimics of copper oxidases and oxygenases: a theoretical study*, Chem. Eur. J. 4 (1998), pp. 1297–1304.

[13] (a) J. Miralles, J.P. Daudey, and R. Caballol, *Variational calculation of small energy differences. The singlet–triplet gap in $[Cu_2Cl_6]^{-2}$*, Chem. Phys. Lett. 198 (1992), pp. 555–562. (b) J. Miralles, O. Castell, R. Caballol, and J.P. Malrieu, *Specific CI calculations of energy differences. Transition energies and bond energies*, Chem. Phys. 172 (1993), pp. 33–43.

[14] C.J. Calzado, J.M. Clemente-Juan, E. Coronado, A. Gaita-Arino, and N. Suaud, *Role of the electron transfer and magnetic exchange interactions in the magnetic properties of mixed-valence polyoxovanadate complexes*, Inorg. Chem. 47 (2008), pp. 5889–5901.

[15] C. de Graaf, C. Sousa, I. de P.R. Moreira, and F. Illas, *Multiconfigurational perturbation theory: an efficient tool to predict magnetic coupling parameters in biradicals, molecular complexes, and ionic insulators*, J. Phys. Chem. A 105 (2001), pp. 11371–11378.

[16] C.J. Calzado, J.F. Sanz, J.P. Malrieu, and F. Illas, Ab initio *systematic determination of the t-J effective Hamiltonian parameters for superconducting Cu-oxides*, Chem. Phys. Lett. 307 (1999), pp. 102–108.

[17] C.J. Calzado, J.F. Sanz, and J.P. Malrieu, *Accurate* ab initio *determination of magnetic interactions and hopping integrals in $La_{2-x}Sr_xCuO_4$ systems*, J. Chem. Phys. 112 (2000), pp. 5158–5167.

[18] N. Suaud and M.B. Lepetit, Ab initio *evaluation of local effective interactions in α-NaV_2O_5*, Phys. Rev. B 62 (2000), pp. 402–409.

[19] N. Suaud and M.B. Lepetit, Ab initio *evaluation of the charge ordering in α-NaV_2O_5*, Phys. Rev. Lett. 88 (2002), 056405.

[20] J. Cabrero, N. Ben Amor, C. de Graaf, F. Illas, and R. Caballol, Ab initio *study of the exchange coupling in oxalato-bridged Cu(II) dinuclear complexes*, J. Phys. Chem. A 104 (2000), pp. 9983–9989.

[21] C.J. Calzado, J. Cabrero, J.P. Malrieu, and R. Caballol, *Analysis of the magnetic coupling in binuclear complexes. I. Physics of the coupling*, J. Chem. Phys. 116 (2002), pp. 2727–2747.

[22] C.J. Calzado, J. Cabrero, J.P. Malrieu, and R. Caballol, *Analysis of the magnetic coupling in binuclear complexes. II. Derivation of valence effective Hamiltonians from* ab initio *CI and DFT calculations*, J. Chem. Phys. 116 (2002), pp. 3985–4000.

[23] N. Suaud, A. Gaita-Arino, J.M. Clemente-Juan, J. Sanchez-Marin, and E. Coronado, *Electron delocalization in mixed-valence Keggin polyoxometalates.* Ab initio *calculation of the local effective transfer integrals and its consequences on the spin coupling*, J. Am. Chem. Soc. 124 (2002), pp. 15134–15140.

[24] E. Bordas, C. de Graaf, R. Caballol, and C.J. Calzado, *Electronic structure of $CaCu_2O_3$: spin ladder versus one-dimensional spin chain*, Phys. Rev. B 71 (2005), 045108.

[25] J. Chalupsk, F. Neese, E.I. Solomon, U. Ryde, and L. Rulek, *Multireference* ab initio *calculations on reaction intermediates of the multicopper oxidases*, Inorg. Chem. 25 (2006), pp. 11051–11059.

[26] B. Le Guennic, S. Petit, G. Chastanet, G. Pilet, N. Ben Amor, and V. Robert, *Antiferromagnetic behavior based on quasi-orthogonal MOs: synthesis and characterization of a Cu3 oxidase model*, Inorg. Chem. 47 (2008), pp. 572–577.

[27] Z. Barandiarán and L. Seijo, *The* ab initio *model potential method – Cowan-Griffin relativistic core potentials and valence basis-sets from Li(Z = 3) to La(Z = 57)*, Can. J. Chem. 70 (1992), pp. 409–415.

[28] CASDI program, N. Ben Amor, and D. Maynau, *Size-consistent self-consistent configuration interaction from a complete active space*, Chem. Phys. Lett. 286 (1998), pp. 211–220.

[29] C.J. Calzado and J.P. Malrieu, Ab initio *determination of an extended Heisenberg Hamiltonian in CuO_2 layers*, Eur. Phys. J. B 21 (2001), pp. 375–381.

[30] I. de P.R. Moreira and F. Illas, *A unified view of the theoretical description of magnetic coupling in molecular chemistry and solid state physics*, Phys. Chem. Chem. Phys. 8 (2006), pp. 1645–1659.

[31] E. Bordas, R. Caballol, C. de Graaf, and J.P. Malrieu, *Toward a variational treatment of the magnetic coupling between centres with elevated spin moments*, Chem. Phys. 309 (2005), pp. 259–269.

[32] C. de Graaf, L. Hozoi, and R. Broer, *Magnetic interactions in sodium and calcium vanadates*, J. Chem. Phys. 120 (2004), pp. 961–967.

[33] C.J. Calzado, C. de Graaf, E. Bordas, R. Caballol, and J.P. Malrieu, *Four-spin cyclic exchange in spin ladder cuprates*, Phys. Rev. B 67 (2003), 132409.

[34] N. Suaud, A. Gaita-Ariño, J.M. Clemente-Juan, and E. Coronado, *Electron delocalization and electrostatic repulsion at the origin of the strong spin coupling in mixed-valence Keggin polyoxometalates:* ab initio *calculations of the one- and two-electron processes*, Chem. Eur. J. 10 (2004), pp. 4041–4053.

[35] C. Bloch, *Sur la theorie des perturbations des etats lies*, Nucl. Phys. 6 (1958), pp. 329–347.

[36] J. Cabrero, C. de Graaf, E. Bordas, R. Caballol, and J.-P. Malrieu, *Role of the coordination of the azido bridge in the magnetic coupling of copper(II) binuclear complexes*, Chem. Eur. J. 9 (2003), pp. 2307–2315.

[37] (a) J.B. Goodenough, *Theory of the role of covalence in the perovskite-type manganites [La,M(II)]MnO$_3$*, Phys. Rev. 100 (1955), pp. 564–573. (b) J.B. Goodenough, *Magnetism and Chemical Bond*, Interscience, New York, 1963. (c) J. Kanamori, *Superexchange interaction and symmetry properties of electron orbitals*, J. Phys. Chem. Solids 10 (1959), pp. 87–98.

[38] E. Ruiz, C. de Graaf, P. Alemany, and S. Alvarez, *Further theoretical evidence for the exceptionally strong ferromagnetic coupling in oxo-bridged Cu(II) dinuclear complexes*, J. Phys. Chem. A 106 (2002), pp. 4938–4941.